DOI: 10.1002/ange.201308545

Porphyrinoids

Modulation of Dual Electronic Circuits of [26]Hexaphyrins Using Internal Aromatic Straps**

Hirotaka Mori, Jong Min Lim, Dongho Kim, and Atsuhiro Osuka**

Annulene chemistry has played a central role in understanding the relationship between the structural and electronic characteristics and aromaticity so far.[1] As an important and intricate class, annuleno(annulenes), that is, annulenes fused to other annulenes have been demonstrated to have a more elaborate bicyclic macrocycle with dual-potential electronic networks, pointing to their potentials to serve as a three-dimensionally extended aromatic and/or antiaromatic system and a switching functional motif.

In recent years, expanded porphyrins have emerged as a new class of azaannulene variants which are highly conjugated, have versatile electronic states, and show facile redox reactions.[2] In particular, the electronic networks of *meso*-aryl expanded porphyrins bear sets of regularly arranged pyrrolic nitrogen atoms, allowing multi-metal coordination,[3] protonation-induced conformational change, for example, from a Hückel conformation to a Möbius conformation,[4] and facile redox interconversion with maintenance of molecular neutrality. Despite these promising attributes, annuleno(annulene)-type expanded porphyrins with a dual conjugated network have remained almost unexplored so far. As rare examples, internally bridged expanded porphyrins such as 1,4-phenylene-bridged octaphyrin and decaphyrin[5a] and vinylene-bridged hexaphyrins[5b] have been explored but the participation of the internal bridge in the expanded porphyrin (global) network is minimal because of the almost perpendicular arrangement of the bridge with regard to the expanded porphyrin. Quite recently, 2,5-thienylene-strapped [26]dithiahexaphyrin was reported as a potential example to show a dual conjugation of [18]dithiaporphyrin and/or [26]dithiahexaphyrin.[6] However, it has remained unclear what structural elements are important to determine the effective electronic network of dual conjugation. With this in background, we embarked on exploration of aromatic strapped [26]hexaphyrins by changing the aromatic strap.

Here, we report the synthesis and characterization of [26]hexaphyrins **1**, **2**, and **3** (Figure 1) with an aromatic strap

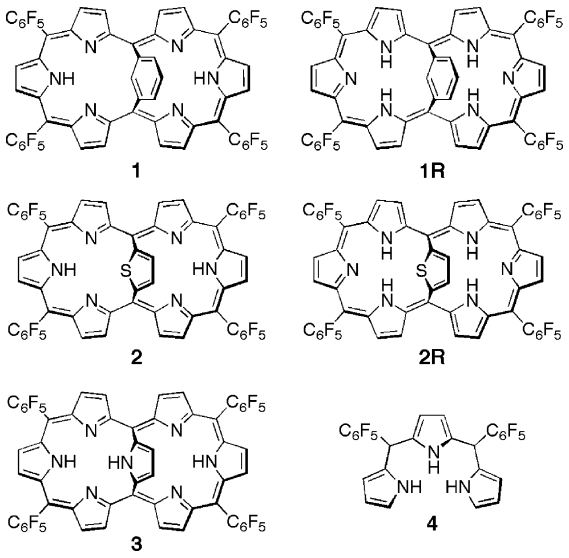

Figure 1. Internally aromatic strapped hexaphyrins **1**, **2**, and **3**, and tripyrromethane **4**.

in 5,20 position. In all cases, the hexaphyrin frameworks consist of six pyrroles. Tripyrromethane **4** was condensed with 1,3-diformylbenzene in a 2:1 ratio, and the resulting mixture was subsequently oxidized with 2,3-dichloro-5,6-dicyano-1,4-benzoquinone (DDQ). Separation over a silica gel column gave 1,3-phenylene-strapped [26]hexaphyrin **1** in 13% yield. 2,5-Thienylene- and 2,5-pyrrylene-strapped [26]hexaphyrins **2** and **3** were similarly prepared from condensations of **4** with 2,5-diformylthiophene and 2,5-diformylpyrrole in 20 and 14% yields, respectively.[7] High-resolution electrospray ionization time-of-flight mass measurements displayed the parent ion peaks at the expected positions (see the Supporting Information).

The structures of **1**, **2**, and **3** have been revealed by single-crystal X-ray diffraction analysis, although the reflection data for **3** are not good enough to discuss the bond length. [26]Hexaphyrins **1**, **2**, and **3** have been all shown to take bent dumbbell-like conformations of the hexaphyrin network, over which the aromatic groups are strapped (Figure 2). The

[*] H. Mori, Prof. Dr. A. Osuka
Department of Chemistry, Graduate School of Science
Kyoto University, Sakyo-ku, Kyoto 606-8502 (Japan)
E-mail: osuka@kuchem.kyoto-u.ac.jp
Dr. J. M. Lim, Prof. Dr. D. Kim
Spectroscopy Laboratory for Functional*p*-Electronic Systems and
Department of Chemistry, Yonsei University
Seoul 120-749 (Korea)
E-mail: dongho@yonsei.ac.kr

[**] The work at Kyoto was supported by Grants-in-Aid from MEXT (grant number 25220802 (S)) for Scientific Research. The work at Yon-sei was supported by the Midcareer Researcher Program of the Ministry of Education, Science, and Technology (MEST) of Korea (grant number 2010-0029668). Support from the Global Research Laboratory (GRL) Program of the Ministry of Education, Science, and Technology (MEST) of Korea (grant number 2013-8-1472) is acknowledged. H.M. acknowledges a JSPS Fellowship for Young Scientists.

Supporting information for this article is available on the WWW under http://dx.doi.org/10.1002/anie.201308545.

 © 2013 Wiley-VCH Verlag GmbH & Co. KGaA, Weinheim

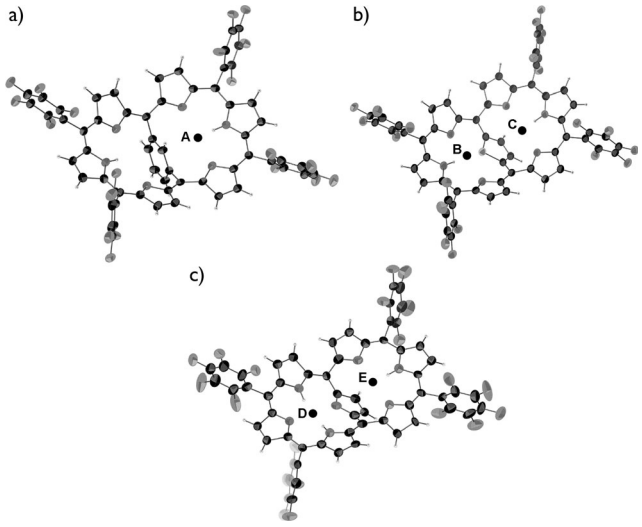

Figure 2. X-ray crystal structure of a) **1**, b) **2**, and c) **3**; only one of the two molecules in the unit cell is shown for all cases. Solvent molecules are omitted for clarity. The thermal ellipsoids represent a probability level of 30%.

hexaphyrin networks consist of two planar tripyrromethene subunits that are bent at 5-, and 20-strapping positions with angles of 18(14)°, 29(25)°, and 14(13)°, respectively (see the Supporting Information).[7,8] The 1,3-phenylene strap in **1** is tilted almost perpendicular with regard to the hexaphyrin framework, suggesting its little involvement in the conjugation and thus dominant contribution of [26]hexaphyrin network. The dihedral angles of the 1,3-phenylene strap toward the tripyrromethene unit are 85(86)° (Figure 2a). On the other hand, the 2,5-thienylene group in **2** and the 2,5-pyrrylene group in **3** are strapped in a more parallel manner with small dihedral angles of 31.2(35.6)° and 18.9(13.4)°, respectively (Figure 2b and c). These structural features lead to more planar arrangements of [18]thiaporphyrin network in **2** with mean plane deviations (0.341 and 0.409 Å) and [18]porphyrin network in **3** with mean plane deviations (0.411 and 0.414 Å). Interestingly, the C2(α)-C3(β) bond distance in the 2,5-thienylene bridge in **2** is 1.404(1.410) Å, being distinctly longer than that of C3(β)-C4(β′), 1.362-(1.367) Å, indicating a significant contribution of [18]thiaporphyrin network (Scheme 1a, resonance contributor **2B**).

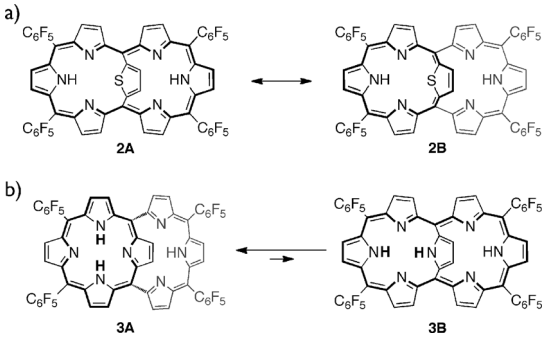

Scheme 1. a) Possible resonance in **2** and b) possible tautomeric equilibrium of **3**. The effective conjugation is indicated by bold lines.

The cyclic voltammetry of **1**–**3** performed in CH_2Cl_2 versus ferrocene/ferrocenium cation (see the Supporting Information) indicated reversible reduction waves at −0.72 and −0.99 V for **1**, −0.77 and −0.98 V for **2**, and −0.78 and −1.04 V, for **3**, respectively. Reversibility and potential value and potential differences between the first and second reduction waves are similar to those of planar aromatic [26]hexaphyrins, suggesting the effective [26]hexaphyrin network in electrochemical response.

Despite the similarities in the strapped dumbbell structures and the electrochemical responses, the absorption and fluorescence spectra of **1**, **2**, and **3** are radically different (Figure 3). The UV/Vis absorption spectrum of **1** exhibits

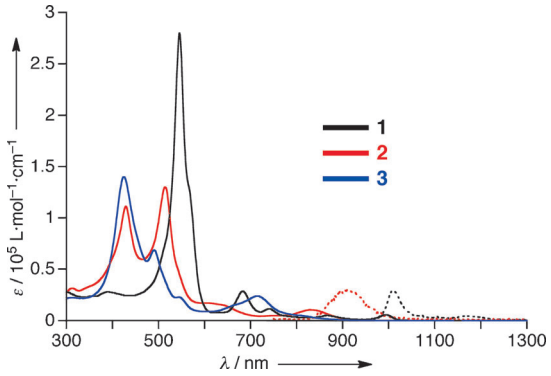

Figure 3. UV/Vis/NIR absorption and fluorescence spectra of **1**, **2**, and **3** in CH_2Cl_2.

a sharp Soret-like band at 546 nm and Q-like bands at 683, 741, 867, and 994 nm, which are similar to those of dumbbell-like aromatic [26]hexaphyrins such as internally vinylene-bridged [26]hexaphyrin[5b] and *meso*-free tetraaryl[26]hexaphyrin.[10] The well-structured fluorescence was observed for **1** in the NIR spectral region at 1010 nm with a Stokes shift of 99 cm^{-1} (see the Supporting Information). The observed Stokes shift of **1** is smaller than that (171 cm^{-1}) of the parent hexakis(pentafluorophenyl) [26]hexaphyrin.[10] These data indicate a predominant contribution of the [26]hexaphyrin network and a small structural change in the excited-state of **1**. In contrast, the UV/Vis absorption spectrum of **2** shows two Soret-like bands at 429 and 515 nm, which may correspond to those of [18]thiaporphyrin and [26]hexaphyrin chromophores, respectively, and the fluorescence spectrum was observed as a weak and structureless band around 910 nm. The observed large Stokes shift of **2** (954 cm^{-1}) indicates large structural changes in its excited-state. The UV/Vis absorption spectrum of **3** shows a characteristic porphyrin Soret-like band at 425 nm with shoulders at 491 and 545 nm and a broad Q-like band in the range of 600–950 nm, suggesting predominant contribution of an [18]porphyrin network. Different from **1** and **2**, hexaphyrin **3** does not emit fluorescence.

The ^{1}H NMR spectrum of **1** at 25 °C indicates its symmetric structure by showing three signals for the outer β-pyrrolic protons in the range of 9.94–8.55 ppm, a broad singlet for the inner pyrrolic protons at −1.83 ppm, and three separate signals for the bridging 1,3-phenylene unit at 4.27,

© 2013 Wiley-VCH Verlag GmbH & Co. KGaA, Weinheim

3.46, and −3.42 ppm. These data help us to assign the main conjugation circuit of **1** as a typical Hückel aromatic [26]hexaphyrin. Actually, the harmonic oscillator model of aromaticity (HOMA) value in the packing structure and the nucleus-independent chemical shifts (NICS) in the optimized structure were calculated to be 0.645 (0.739) and −15.85 ppm at point A (Figure 2a). [26]Hexaphyrin **1** was quantitatively reduced with $NaBH_4$ to corresponding [28]hexaphyrin **1R** that is a certainly stable antiaromatic molecule. The ^{1}H NMR spectrum of **1R** shows a broad signal for the pyrrolic NH proton at 20.69 ppm, sharp peaks for the 1,3-phenylene bridge at 17.00, 11.41, and 10.62 ppm, and peaks for the outer β-pyrrolic protons in the range of 4.45–3.99 ppm (see the Supporting Information). The observed large paratropic ring current for **1R** is thought to be arising from its planar hexaphyrin structure enforce by the 1,3-phenylene bridge.

The ^{1}H NMR spectrum of **2** at 25 °C displays three signals for the outer β-protons at 9.82 (4H) and 8.67 (8H) ppm, a broad singlet for the inner pyrrolic protons at −0.91 ppm, indicating an obvious diatropic ring current arising from the [26]hexaphyrin conjugation network. Importantly, a peak for the 3,4-thienylene protons was observed at 4.26 ppm. Considering the strong diatropic ring current of the [26]hexaphyrin network and the location of the thienylene strap, this chemical shift probably indicates a non-negligible diatropic ring current of the local [18]thiaporphyrin circuit (Scheme 1, **2B**). Hence, the dual contribution of [26]hexaphyrin and [18]thiaporphyrin is conceivable for **2**. Actually, the HOMA values have been calculated to be 0.802(0.646) for the [18]thiaporphyrin network and 0.664(0.631) for the [26]hexaphyrin network. Both values are well within the range of aromatic porphyrinoids. The NICS(0) values on the optimized structure also support this hypothesis, exhibiting −12.80 and −10.93 ppm at points B and C, respectively (Figure 2b). Reduction of **2** with $NaBH_4$ gave **2R**, which again displays antiaromatic properties. Remarkably, the ^{1}H NMR spectrum of **2R** at −60 °C displays signals for the inner NH protons and 3,4-thienylene protons at 32.27 and 17.18 ppm, respectively, and signals for the outer β-pyrrolic protons at 1.77, 1.30, and 1.20 ppm, indicating a stronger paratropic ring current than that of **1R. 2R** is more easily oxidized back to **2** as compared with **1R**.

The ^{1}H NMR spectrum of **3** is rather broad at room temperature but becomes sharp at −60 °C, showing two sets of signals in a ratio of 12:1. The major and minor sets show nonsymmetric and symmetric spectral patterns, respectively. The major set has been assigned to structure **3A** in which a [18]porphyrin conjugation network is dominant and the rest tripyrramethene strap does not contribute to the [26]hexaphyrin conjugation. Characteristically, signals of the peripheral pyrrolic protons at the porphyrin part are observed in the range of 8.68–9.94 ppm, and a signal for the inner pyrrolic NH group appears at −0.48 ppm, while signals for the appended tripyrromethene unit are observed at 8.00, 7.42, 5.79, and 5.74 ppm, and one singlet for the inner pyrrolic NH group appears at 5.79 ppm. In contrast, the ^{1}H NMR spectral pattern of the minor set is similar to those of **1** and **2**, featuring signals for the outer β-H in the range of 9.11–10.59 ppm, a broad signal for the inner NH at −0.98, and one singlet by the β-H of the bridging pyrrylene unit at −5.45 ppm. The minor set has been assigned to structure **3B** (Scheme 1b). Additionally, the anisotropy of induced current density (AICD) calculation of the optimized structures, **3A** and **3B** revealed porphyrin- and hexaphyrin-like conjugation pathways, respectively (see the Supporting Information). Different from **1** and **2**, reduction of **3** with $NaBH_4$ was sluggish, giving an intractable mixture, probably because of the electron-rich nature of the pyrrylene strap. The theoretical calculation at B3LYP/6-31G(d) level on the basis of the optimized structures by the Gaussian program revealed that the structure **3A** is more stable than the structure **3B** by 0.95 kcal mol^{-1} ([**3B**]/[**3A**] = 0.11 at −60 °C), which is consistent with the observed equilibrium ([**3B**]:[**3A**] = 12:1 at −60 °C). The observed preference of structure **3A** may be ascribed to an energy gain provided by effective intramolecular hydrogen bonding, for which the planar porphyrin structure is important, hence leaving the tripyrromethene out of the porphyrin plane to induce the unsymmetrical structure.

Furthermore, the photophysical properties of **1**, **2**, and **3** have been examined by femtosecond transient absorption (TA) spectroscopy. The singlet-excited-state lifetime of **1** was estimated to be 158 ps (Figure 4a). The TA spectral features of **1**, such as relative signal intensities between ground-state bleaching and excited-state absorption are quite reminiscent of those of typical aromatic [26]hexaphyrins.[11] The TA spectra of **2** differed from those of **1** by featuring a strong bleaching at the Soret-like band of the hexaphyrin part, an absorbance around 570–580 nm, and a broad absorbance at wavelengths longer than 650 nm. A decay component with t = 373 ps was observed at 550 nm but most of the transient absorbance remained in a time window of 3 ns. The TA spectra of **2** have been globally analyzed to identify two principal spectral species, most probably S_1 and T_1 states of **2** (see the Supporting Information), the latter of which was formed by the efficient intersystem crossing (ISC) process from S_1 because of the heavy-atom effect of the sulfur atom at the 2,5-thienylene strap. The efficient heavy-atom effect is consistent with the low fluorescence quantum yield and indicates the significant involvement of the thienylene strap in the conjugation network of **2**. Using a [18]thiaporphyrin (see the Supporting Information), the sulfur heavy-atom effect was confirmed. Actually, the fluorescence lifetime of the [18]thiaporphyrin was determined to be about 1.9 ns (see the Supporting Information), displaying five-fold reduction in S1-state lifetime compared to normal [18]porphyrin. The TA spectra of **3** are radically different from those of **1** and **2**, revealing very short-lived (t = 10 ps) large transient absorbances in the range of 530–600 nm. The short lifetime of the S_1-state is consistent with its nonfluorescent behavior. Characteristic spectral features and photodynamics of [26]hexaphyrin were not detected in the TA spectra of **3**. While the major conjugation network of **3** is thought to be [18]porphyrin, its photoexcited behavior is different from usual porphyrins. These spectroscopic features may originate from the complex electronic communication between the [18]porphyrin-like network and the appended tripyrromethene unit or the involvement of ultrafast pyrrolic NH tautomerism.

 © 2013 Wiley-VCH Verlag GmbH & Co. KGaA, Weinheim

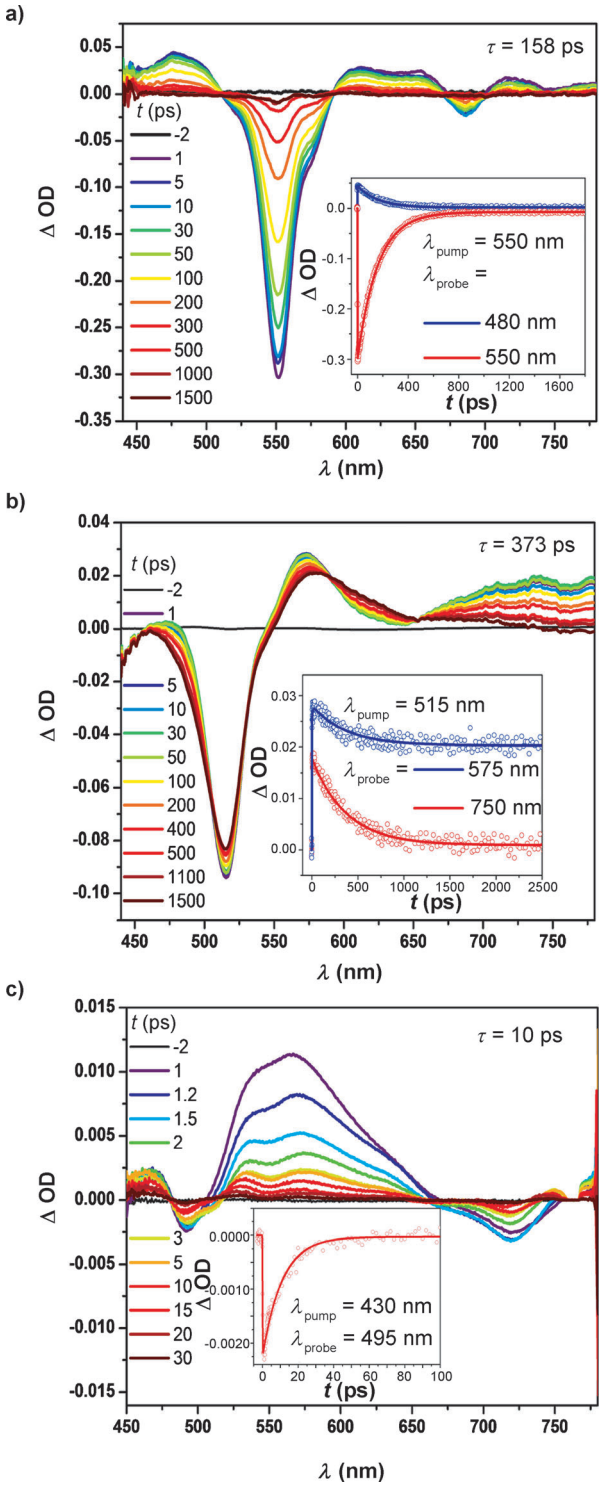

Figure 4. Femtosecond transient absorption spectra and decay profiles of **1**, **2**, and **3** in toluene.

In summary, the internally aromatic strapped [26]hexaphyrins **1**, **2**, and **3** were prepared as three-dimensionally extended porphyrinoids[12] and showed dual electronic networks. The effective conjugation networks of these hexaphyrins can be modulated by internal aromatic straps. The [26]hexaphyrin network is predominant for **1** because of the negligible involvement of the 1,3-phenylene strap. The active involvement of the 2,5-thienylene and 2,5-pyrrylene straps in the macrocyclic conjugation causes roughly equal contribution of [26]hexaphyrin and [18]thiaporphyrin for **2** and predominant contribution of [18]porphyrin for **3**. Investigations of more elaborated expanded porphyrins with two or more conjugation networks are actively pursued in our laboratory.

Received: October 1, 2013
Published online: November 11, 2013

Keywords: annulenoannulenes · conjugation · hexaphyrins · internal bridges · porphyrinoids

[1] a) M. Nakagawa, *The Chemistry of Annulenes—From the Standpoint of Organic Chemistry—*, Osaka University Press, Osaka, **1996**; b) M. Nakagawa, *Angew. Chem.* **1979**, *91*, 215; *Angew. Chem. Int. Ed. Engl.* **1979**, *18*, 202.

[2] a) J. L. Sessler, D. Seidel, *Angew. Chem.* **2003**, *115*, 5292; *Angew. Chem. Int. Ed.* **2003**, *42*, 5134; b) H. Furuta, H. Maeda, A. Osuka, *Chem. Commun.* **2002**, 1795; c) T. K. Chandrashekar, A. Venkatraman, *Acc. Chem. Res.* **2003**, *36*, 676; d) S. Shimizu, A. Osuka, *Eur. J. Inorg. Chem.* **2006**, 1319; e) J.-Y. Shin, H. Furuta, K. Yoza, S. Igarashi, A. Osuka, *J. Am. Chem. Soc.* **2001**, *123*, 7190; f) M. Stępień, N. Sprutta, L. Latos-Grażyński, *Angew. Chem.* **2011**, *123*, 4376; *Angew. Chem. Int. Ed.* **2011**, *50*, 4288; g) S. Saito, A. Osuka, *Angew. Chem.* **2011**, *123*, 4432; *Angew. Chem. Int. Ed.* **2011**, *50*, 4342; h) A. Osuka, S. Saito, *Chem. Commun.* **2011**, *47*, 4330.

[3] a) S. Mori, A. Osuka, *J. Am. Chem. Soc.* **2005**, *127*, 8030; b) S. Saito, K. Furukawa, A. Osuka, *Angew. Chem.* **2009**, *121*, 8230; *Angew. Chem. Int. Ed.* **2009**, *48*, 8086; c) Y. Kamimura, S. Shimizu, A. Osuka, *Chem. Eur. J.* **2007**, *13*, 1620.

[4] a) S. Saito, J.-Y. Shin, J. M. Lim, K. S. Kim, D. Kim, A. Osuka, *Angew. Chem.* **2008**, *120*, 9803; *Angew. Chem. Int. Ed.* **2008**, *47*, 9657; b) J. M. Lim, J.-Y. Y. Tanaka, S. Saito, A. Osuka, D. Kim, *J. Am. Chem. Soc.* **2010**, *132*, 3105.

[5] a) V. G. Anand, S. Saito, S. Shimizu, A. Osuka, *Angew. Chem.* **2005**, *117*, 7410; *Angew. Chem. Int. Ed.* **2005**, *44*, 7244; b) M. Suzuki, A. Osuka, *J. Am. Chem. Soc.* **2007**, *129*, 464.

[6] G. Karthik, M. Sneha, V. P. Raja, J. M. Lim, D. Kim, A. Srinivasan, T. K. Chandrashekar, *Chem. Eur. J.* **2013**, *19*, 1886.

[7] One referee wondered about the formation of 1,3-benziporphyrin, thiaporphyrin, or porphyrin in these condensation reactions. But these molecules were not detected or detected in very small amounts.

[8] a) Crystallographic data for **1**: triclinic, space group $P\bar{1}$ (no. 2), $a = 18.8577(3)$, $b = 20.0669(4)$, $c = 20.2441(4)$ Å, $\alpha = 66.1520(8)$, $\beta = 62.6962(8)$, $\gamma = 78.0242(8)$, $V = 6223.7(2)$ Å^3, $T = 93$ K, $\rho_{calcd} = 1.555$ g cm^{-3}, $Z = 2$, $R_1 = 0.0779$ ($I > 2\sigma(I)$), $R_w = 0.2653$ (all data), GOF = 1.046. CCDC 958400 contains the supplementary crystallographic data for this paper. These data can be obtained free of charge from The Cambridge Crystallographic Data Centre via www.ccdc.cam.ac.uk/data_request/cif; b) Crystallographic data for **2**: monoclinic, space group $C2/m$ (no. 12), $a = 18.7976(3)$, $b = 27.6642(5)$, $c = 23.9062(4)$ Å, $\beta = 103.7880(7)°$, $V = 12073.5(4)$ Å^3, $T = 93$ K, $\rho_{calcd} = 1.496$ g cm^{-3}, $Z = 8$, $R_1 = 0.0656$ ($I > 2\sigma(I)$), $R_w = 0.1846$ (all data), GOF = 1.006. CCDC 958401 contains the supplementary crystallographic data for this paper. These data can be obtained free of charge from The Cambridge Crystallographic Data Centre via www.ccdc.cam.ac.uk/data_request/cif; c) Crystallographic data for **3**: monoclinic, space group $P2_1/a$ (no. 14), $a = 17.2023(3)$, $b =$

© 2013 Wiley-VCH Verlag GmbH & Co. KGaA, Weinheim

34.7013(6), $c = 17.8053(3)$ Å, $\beta = 110.3636(8)°$, $V = 9964.5(3)$ Å^3, $T = 93$ K, $\rho_{calcd} = 1.711$ g cm^{-3}, $Z = 4$, $R_1 = 0.1511$ ($I > 2\sigma(I)$), $R_w = 0.4395$ (all data), GOF = 1.099. CCDC 958402 CCDC 6.. contains the supplementary crystallographic data for this paper. These data can be obtained free of charge from The Cambridge Crystallographic Data Centre via www.ccdc.cam.ac.uk/data_request/cif.

[9] The unit cell contained two different hexaphyrins. Thus, two structural parameters are given for **1**–**3**.

[10] T. Koide, G. Kashiwazaki, M. Suzuki, K. Furukawa, M.-C. Yoon, S. Cho, D. Kim, A. Osuka, *Angew. Chem.* **2008**, *120*, 9807; *Angew. Chem. Int. Ed.* **2008**, *47*, 9661.

[11] Z. S. Yoon, J. H. Kwon, M.-C. Yoon, M. K. Koh, S. B. Noh, J. L. Sessler, J. T. Lee, D. Seidel, A. Aguilar, S. Shimizu, M. Suzuki, A. Osuka, D. Kim, *J. Am. Chem. Soc.* **2006**, *128*, 14128.

[12] Pyrrylene-based three-dimensional or bicyclic systems: a) A. Andrievsky, F. Ahuis, J. L. Sessler, F. Vögtle, D. Gudat, M. Moini, *J. Am. Chem. Soc.* **1998**, *120*, 9712; b) C. Bucher, R. S. Zimmerman, V. Lynch, J. L. Sessler, *J. Am. Chem. Soc.* **2001**, *123*, 9716.

 © 2013 Wiley-VCH Verlag GmbH & Co. KGaA, Weinheim